



ISSN: 0067-2904

Synthesis of Silver Nanoparticles Using *L.Rosa* Flowers Extracts: Thermodynamic and Kinetic Studies on the Inhibitory Effects of Nanoparticles on Creatine Kinase Activity

Riyam Lateef Khalaf *, Elham Majeed Ahmed, Thikra Hasan Mathkor
Hadeel Y.AL-Zubaidi

Department of Chemistry, College of Science, University of Baghdad, Al-Jadria, Baghdad, IRAQ

Received: 13/8/2020

Accepted: 10/2/2021

Abstract

The present work investigates the synthesis of silver nanoparticles (AgNPs) by a biological method using *L.Rosa* flower extract and silver nitrate as precursors. Optimum conditions of synthesis were studied, such as pH, temperature, concentration of extract, concentration of silver nitrate, and stability with time. Characterization of AgNPs was carried out using UV-visible Spectroscopy, Scanning Electron Microscopy, X-Ray Diffraction, Fourier Transform Infrared and Transmission Electron Microscopy. The biosynthesized AgNPs exhibited inhibitory effects on creatine kinase activity in the sera of patients with myocardial infarction, compared with control subjects. Thermodynamic and kinetic studies of creatine kinase were performed. Further studies on other biological activities were performed to exploit AgNPs full potential. In conclusions, the present study utilize a simple, cheap and environmentally green method to synthesize silver nanoparticles. This single step procedure is more suitable for large scale production as it is rapid and eliminates the elaborate processes employed in the other bio-based protocols (e.g. by using fungi and bacteria).

Keywords: Silver nanoparticles, *L.Rosa* extract, green synthesis, creatine kinase, antibacterial activity.

تخليق دقائق الفضة النانوية باستخدام مستخلص ازهار الجوري ودراسة الخواص الترموديناميكية والحركية لتثبيط دقائق الفضة لانزيم كرياتين كيناز

ريام لطيف خلف* ، الهام مجيد احمد ، نكري حسن ، هديل يحيى عبد الرضا

قسم الكيمياء، كلية العلوم، جامعة بغداد، الجادرية، بغداد، العراق

الخلاصة

في هذا العمل تم تخليق دقائق الفضة النانوية بالطريقة البايولوجية باستخدام مستخلص ازهار الجوري ونواتر الفضة. تم دراسة الظروف المثلى للتخليق كالحامضية، درجات الحرارة، تركيز المستخلص، تركيز النترات والاستقرارية مع الوقت اما دقائق الفضة النانوية المحضرة فتم تشخيصها بعدة تقنيات منها مطياف الاشعة فوق البنفسجية (UV-Visible) ولمعرفة المجاميع التي ادت الى اختزال دقائق الفضة بواسطة تقنية FT-IR ولتشخيص حجم وشكل الدقائق المتكونة باستخدام المجهر الالكتروني النافذ والماسح. تم دراسة

*Email: Riyoma92@gmail.com

الحركية والثرموديناميكية لتأثير الدقائق المحضرة على فعالية الانزيم ودراسة تأثير دقائق الفضة النانوية المحضرة بايولوجيا و تأثيرها على فعالية انزيم كرياتين كايبيز في الامصال للاشخاص الاصحاء والمصابين باحتشاء عضلة القلب وكذلك دراسة الفعالية البايولوجية.

Introduction

Synthesis and characterization of nanoparticles gained considerable research interest due to their large surface area which provides unique properties and potential application as compared to their bulk counterparts [1]. Metal nanoparticles such as those made of Ag, Au, Cu and Pt have been widely synthesized using physical, chemical and biosynthesis methods. Bio-based protocols have been turning into viable alternatives to conventional methods, as they appear to be very simple, low cost and ecofriendly. Many scientists have reported the preparation of AgNPs using different biological sources, including bacteria [2], fungi [3], and plants [4]. The plant-mediated synthesis (e.g. using flowers, roots, leaves, shank, seeds, and fruits) is a green chemistry approach which is emerging as an active area of current nano-biotechnological research because of the very high rate of plant extraction and the lack of the need for specific conditions [5]. This plant-mediated approach leads to the production of more stable nanoparticles with maximum yield [6]. Optimization of different parameters, e.g. temperature, pH, time of reaction, concentration of Ag ion, as well as concentration of plant extract, should be considered when nanoparticles are produced through plant biosynthesis [7]. The applications of silver nanoparticles include, for example, the production of electronic devices, biological tools, and many biological and pharmaceutical products [8]. This is probably due to the stability of the nanoparticles, which are suitable to medical usages. Silver is being widely used as an antimicrobial agent. By modifying the structure and functions of the cell membrane, silver ions may attack a wide range of microbes. Bacteria are destroyed at very low concentrations (less than 1–10 μM) of silver nanoparticles, hence they are being used as a germicide in water cleaning systems [9]. However, there are contradictory reports regarding their antibacterial actions against bacteria. In addition, at higher doses, silver can be toxic to mammalian species and freshwater and aquatic organisms. Remarkably, microscale concentrations of silver do not have any hurtful effects on human beings [10].

Creatine kinase (CK) is an enzyme that plays a central role in the metabolism of high-energy consuming tissues, such as the brain, skeletal muscles, and heart, where it functions as an effective buffering system of cellular adenosine triphosphate (ATP) levels. The test of CK in blood is a cardiac marker used to assist the diagnoses of acute myocardial infarction. The regeneration of ATP by transferring a phosphoryl group from phosphocreatine to adenosine diphosphate (ADP) is a reaction that is catalyzed by CK. It has been recognized that the reduction in CK activity may lead to energy homeostasis impairment and, consequently, cell death [11]. Silver nanoparticles showed cytotoxic effects through the interaction between silver ions and sulphhydryl groups of proteins or enzymes (e.g. creatine kinase) [12]. The aim of the present work is to synthesize silver nanoparticles using *L.Rosa* flowers extract and study their biological impacts through the evaluation of their antibacterial activity against gram positive bacteria (e.g. *staphococcus aureus*) and gram negative bacteria (e.g. *Escherichia coli*). Also, we aim to study the effects of AgNPs on creatine kinase activity in sera of patients with myocardial infarction.

Materials and Methods

Materials

Silver nitrate (the stock solution) was acquired from Sigma-Aldrich chemicals and used as received. All glasses were rinsed with diluted nitric acid and deionized water three times before use [13], then dried in hot oven. A stock solution of AgNO_3 (2×10^{-2} M) was prepared by dissolving 0.34 g in 100 ml deionized water. The plant extract 5% (w/v) was prepared by boiling 5.0 g of the powder of fresh *L.Rosa* flowers (collected from the campus of the University of Baghdad, college of science, AL-Jadiria, Baghdad, Iraq) with 100 ml of deionized water for 15 min at 70 °C with stirring. Then, filtration was performed to get the extract by using filter paper. The filtrate of the extract was stored in the dark at 2 °C to be used as a reducing agent [14].

Synthesis of silver nanoparticles

One ml of plant extract (5%) of *Rosa* flowers was added slowly to 2 ml of the stock solution 2×10^{-2} M silver nitrate. After completing the volume to 20 ml with deionized water, the sample was stirred

with heating for one hour at 70 °C. After that, its maximum absorbance was measured using UV-Visible spectrophotometer. The reduction of Ag⁺ to Ag⁰ nanoparticles was indicated by the alteration in color of the solution from yellow to brownish yellow and finally deep brown. This process was affected by several parameters, such as flower extract concentration, AgNO₃ concentration, temperature, pH value, contact time, and stability with time. The sample was washed with distilled water twice then dried to obtain the synthesized silver nanoparticles for characterization.

Optimization conditions of the synthesis of silver nanoparticles

To optimize different conditions of the plant extract-mediated AgNPs synthesis method, the maximum absorbance was recorded at each optimization experiment using UV-visible spectrophotometry.

pH optimization

The optimum pH of the reaction was maintained over different ranges and adjusted by using 0.1 N HCl and 0.1 N NaOH.

Time optimization

The contact time of the reaction was optimized by using different time periods. The reaction time was monitored at 0, 15, 30, 45, 60, 75, 90, 105 and 120 min with stirring and heating at 70 °C for 1, 2, 3, 4, 5, 6 and 7 days. The mixture was then stored in dark at room temperature [15].

Concentration of silver nitrate solution

The concentration of AgNO₃ was optimized, where the reaction was maintained at 0.5, 1, 1.5, 2.0, 2.5 and 3.0 milliliters of AgNO₃ (2 × 10⁻² M) and 2 milliliters of a constant concentration of flowers extract (5%) [16].

Concentration of flowers extract

Similarly, the concentration of flowers extract was optimized by increasing the volume (0.25, 0.50, 0.75, 1.0, 1.25 and 1.50 ml) of 5% flower extract with two milliliters of the constant concentration of AgNO₃ (2 × 10⁻²), then the volume was completed to 20 ml with deionized water [17]

Stability study

After the optimization of the various conditions for AgNPs-plant reaction, the solution was kept in the dark at room temperature and the stability of the synthesized particles was monitored for up to 60 days.

Characterizations of silver nanoparticles

Ultraviolet-visible absorption spectra were recorded at 37°C using a Shimadzu UV-1800 spectrophotometer. A drop of the solution containing the nanoparticles was deposited on a Cu grid covered with amorphous carbon. An aliquot of plant extract filtrate containing silver nanoparticles was tested for scanning electron microscopy (SEM) using SEM S-4160. X-ray diffraction (XRD) pattern was obtained using a Shimadzu XRD-6000 diffractometer with Cu K,α (λ= 1.54056 Å) to confirm the green synthesis of AgNPs. Fourier transform infrared (FTIR) spectra were recorded at 37°C on a Shimadzu FTIR 84005 spectrophotometer. To prepare a sample for FT-IR, the plant extract with AgNPs was dried at 60 °C for one hour, then mixed with suitable amount of KBr. Morphology of silver nanoparticles was examined using Atomic Force Microscope (AFM, Model AA300 Angstrom advanced). Transmission electronic microscopy (TEM) study was performed using a Carl Zeiss EM 900.

Anti-bacterial activity

Testing the activity of AgNPs as anti-bacterial agent was adjusted using the well diffusion method [18] for *Staphylococcus aureus* and *Escherichia coli*. Brain heart infusion (BHI) broth was used to subculture the bacteria which was incubated at 37°C for 24 h. The pathogenic bacterial strains were incubated in Mueller-Hinton agar plates. Sterile paper disks of 5mm diameter saturated with plant extract, as control, and different concentrations of the synthesized silver nanoparticles were placed in each plate. Plates were then incubated for 24 hours at 37°C. The inhibition zones were measured and tabulated.

Effects of AgNPs on CK activity

Effects of AgNPs on the activity of creatine kinase was examined. The study was conducted during the period of May 2018 to June 2018 on blood samples from 20 patients with myocardial disease (8-50 years old) admitted to the medical city hospital, Baghdad, where they were diagnosed with myocardial infarction. Twenty healthy individual (20-45 years old) were included as a control group, with the exclusion of any patient with myocardial disease. After one-hour of diagnosis with

myocardial diseases, venous blood was collected and allowed to clot at room temperature for 30 minutes. Then, the samples were centrifuged for 15 minute to separate the serum. Serum was pipetted and stored at 4 °C until the determination of creatine kinase activity. An assay kit purchased from biolabo- France was utilized for the spectrophotometric measurement of the level of CK. One unit of creatine kinase was defined as the conversion of one micromole of creatine to creatine phosphate per minute at 37 °C and PH 6.8 under specified conditions. 1.5 mL of biosynthesized AgNPs (5%) was added to the sera of each group (patient with myocardial infarction and healthy subjects), then CK activity was determined [19].

Enzyme kinetic and thermodynamic studies

Parameters of creatine kinase in the absence and present of AgNPs were assessed. The reaction mixture was prepared and treated as mentioned in the CK kit assay protocol. CK activity was determined at various constant reactions of creatine phosphate (as a substrate) for the kinetic study. The data of these experiments were used to generate a linear relationship by plotting $1/v$ values against $1/[S]$ values for the control and patient's groups, according to Linweaver-Burk equation [20]. For the thermodynamic study, values of the natural logarithm of the constant of the reaction equilibrium ($\ln K_{eq}$) at different temperatures (20, 30, 37 and 45°C) were plotted against the reciprocal of absolute temperature ($1/T$), according to Van't Hoff equation [21]. The value of ΔH° was calculated from the slope of the resulting straight line.

Results and discussion

In this study, we demonstrated the preparation of silver nanoparticles from *L.Rosa* flowers extract as a reducing, capping, and stabilizing agent. Synthesis of AgNPs was monitored by UV–vis spectra and the reaction was completed within 60 minute with stirring and heating at 70°C. The colorless solution was turned to a brownish red color, which indicates the formation of silver nanoparticles as show in Figure-1.

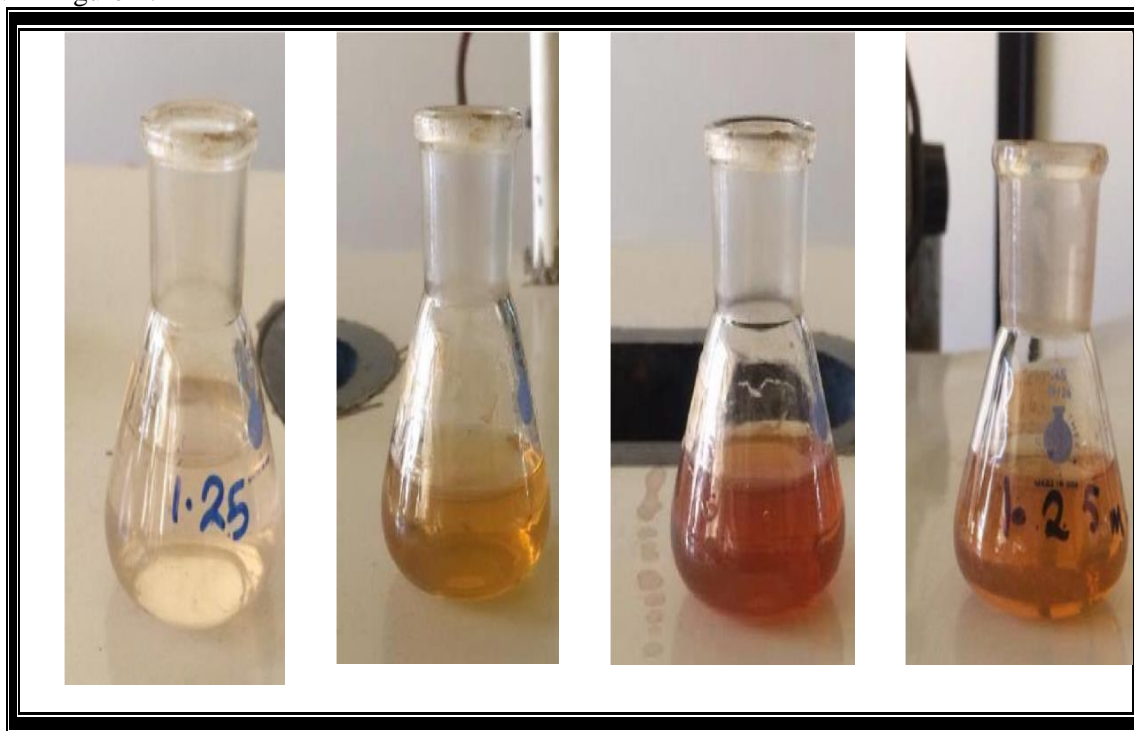


Figure 1- Color change from yellow to brown, which indicates the formation of silver nanoparticles using *L.Rosa* flowers extract with strining and heating at 70 C° for one hour.

Optimization of silver nanoparticles synthesis

Many parameters were optimized for silver nanoparticles preparation, including acidity, stability with time, and concentration variation of $AgNO_3$ and flowers extract.

The value of the pH in the media is one of important factors playing a major role in nanoparticles preparing. As shown in Figure-2, no particle formation was recorded at acidic and alkaline pH, but the maximum peak was absorbed at neutral pH (7), when the AgNPs were synthesized.

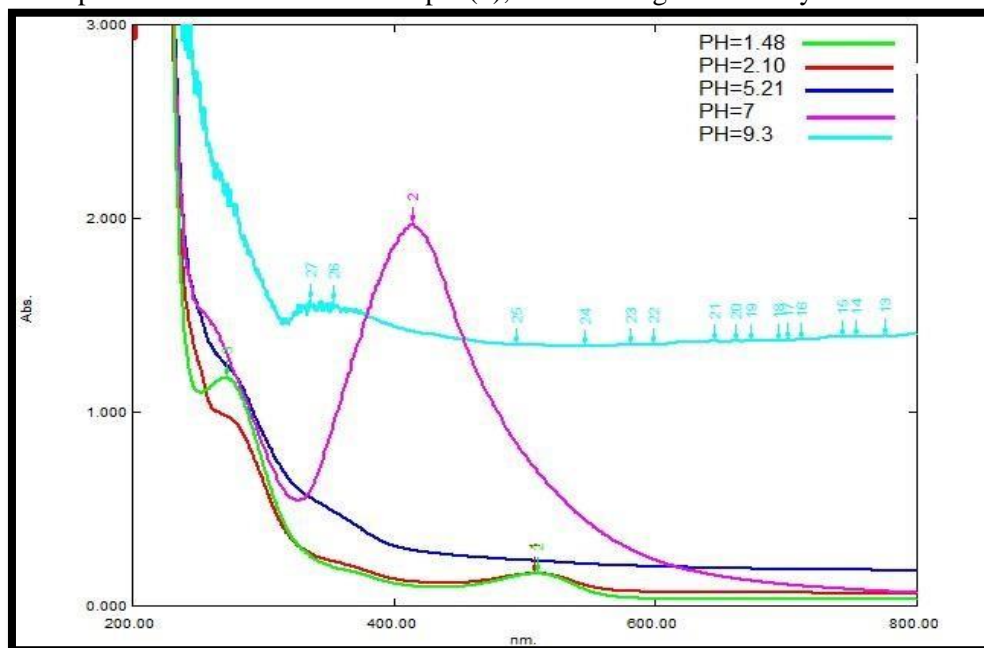


Figure 2- UV-vis spectra of synthesized AgNPs at different pH values, with stirring and heating at 70 °C for one hour.

At optimum pH (7), stability of the synthesized silver nanoparticles was monitored during different time intervals (1 to 7 days). Synthesis of silver nanoparticles was started as the AgNO_3 was added into the reaction. The formation of AgNPs was noticed within 15 minutes and the absorbance was increased with time up to a period of 7 days. The maximum absorption of AgNPs was measured at specified periods of time, as shown in Figure-3.

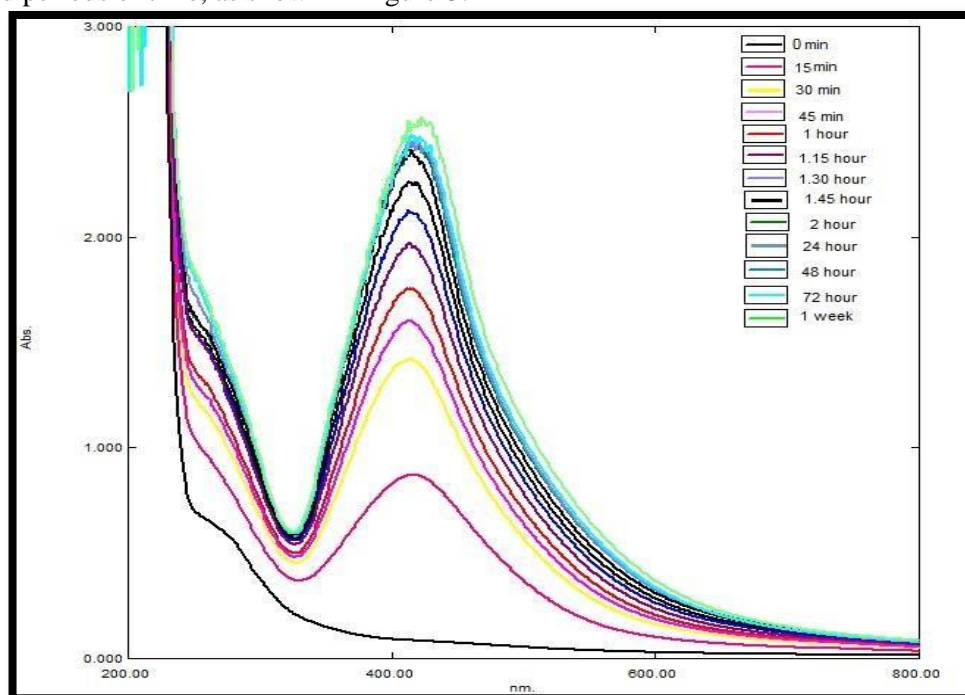


Figure 3- UV-vis spectra of synthesized AgNPs at different time values and pH 7, with stirring and heating at 70 °C.

Furthermore, the characteristics of the in UV–vis absorption spectrum at 422 nm corresponds to the surface plasmon resonance (SPR) of silver nanoparticles. This result confirms previously reported results [22]. The phenomena of SPR occurred at 422 nm at the start of the reaction and it was stabilized in the height and shape of λ_{max} even after the completion of the reaction.

Silver nitrate with volumes of 2 ml or 3 ml supported rapid synthesis of AgNPs, as the peaks with maximum absorption were observed (Figure- 4). Different concentrations of silver nitrate (AgNO_3) were studied for the maximum yield of the synthesized silver nanoparticles.

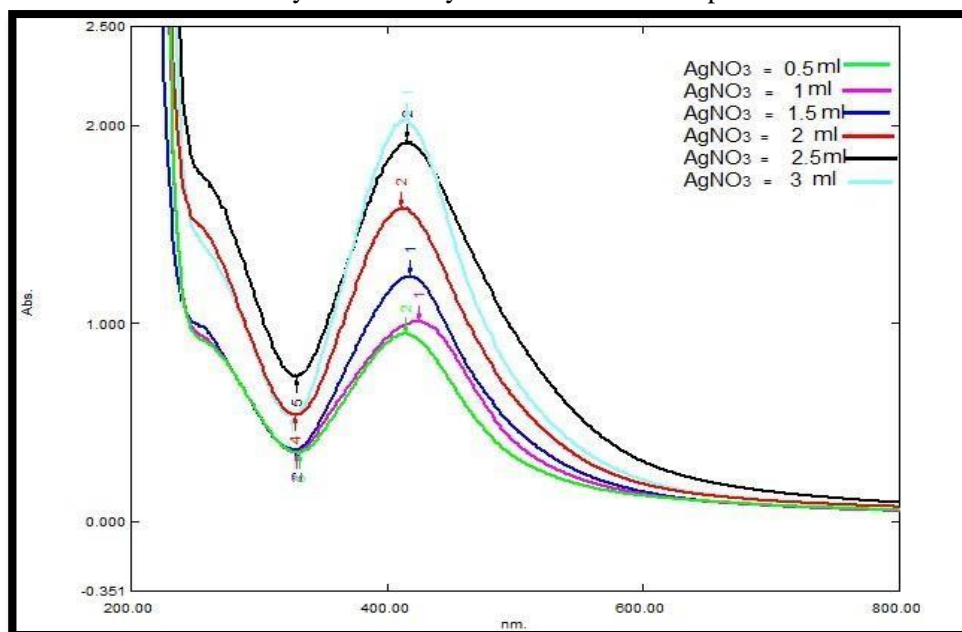


Figure 4- UV–vis spectra of synthesized AgNPs at different concentrations of AgNO_3 and pH 7, with stirring and heating at $70\text{ }^\circ\text{C}$ for one hour.

Similarly, different concentrations of flowers extract were also optimized for the maximum formation of silver nanoparticles. Two milliliters of the constant concentration of silver nitrate was added to different concentrations of flowers extract (0.25, 0.50, 0.75, 1.0, 1.25 and 1.5 ml). As shown in Figure-5, a volume of 1.25 ml of plant extract was sufficient to obtain the highest peak of the synthesized AgNPs, indicating a high yield of (Figure-5).

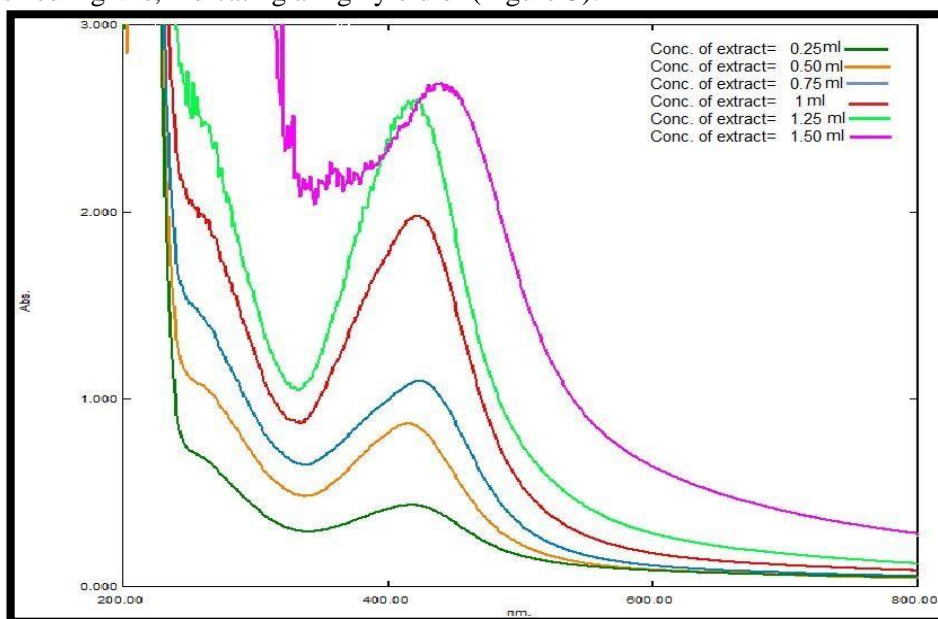


Figure 5- UV–vis spectra of synthesized AgNPs at different concentrations of *L.Rosa* flowers extract and pH 7, with stirring and heating at 70 C° for one hour.

Thus, the optimized medium conditions (pH 7, temp. 70°C, 2 ml volume of silver nitrate and 1.25 mL of *L.Rosa* flowers extracts for 60 min.) supported the maximum production of silver nanoparticles.

To achieve the maximum stability of silver nanoparticles formation at optimized conditions, maximum absorbance of synthesized AgNPs was measured at different periods of storage time (up to two months), as shown in Figure-6. Obviously, there is a slight change in the peak at 422 nm even after two months of storage, indicating the high stability of biosynthesized silver nanoparticles.

The optimized conditions played a major role in the stability and aggregation of the nanoparticles. For better understanding of the mechanism of the reaction, various concentrations of the flowers extract and the substrate were prepared. Many studies indicated that the biomolecules present in the plant extract play an important role in reducing silver ions to the nanosize. It is a chemically complicated phenomenon involving an array of biomolecules, such as enzymes/proteins, flavonoids, phenols, vitamins, organic acids (such as citrates), amino acids and polysaccharides. The flowers of *L. Rosa* were reported to consist of flavonoids, glycosides, and tannins. Quercetin, a well-known flavonol that is found in *L. Rosa* flowers extract, has strong antiviral, antibacterial, anti-inflammatory and anti-carcinogenic effects. Quercetin, isolated alone, was used to synthesize nanoparticles [23]. Hence, we assume that quercetin may be reliable for silver nitrate reduction into silver nanoparticles. However, bio component products or reduced cofactors in plant extracts may also play a crucial role in the reduction of respective salts to nanoparticles.

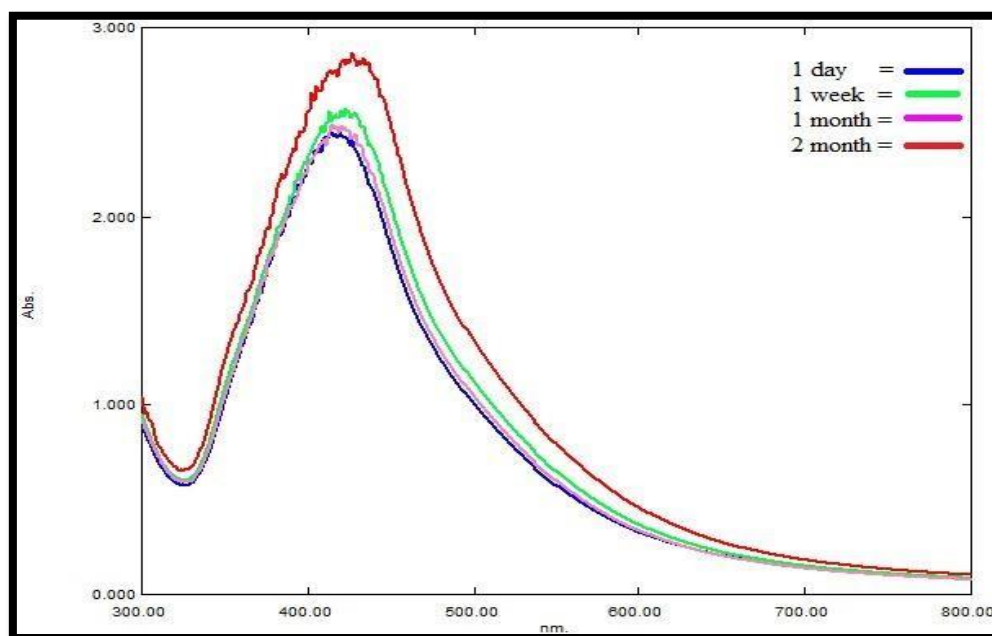


Figure 6- UV-visible spectra of AgNPs stability (1-60 days), formed from *L.Rosa* flowers extract at pH 7 with stirring and heating at 70 C° for one hour.

Characterization of the synthesized silver nanoparticles

The size, shape and distribution of the green-synthesized silver nanoparticles were characterized by TEM in an average size of 7.5 -50 nm (Figure-7).

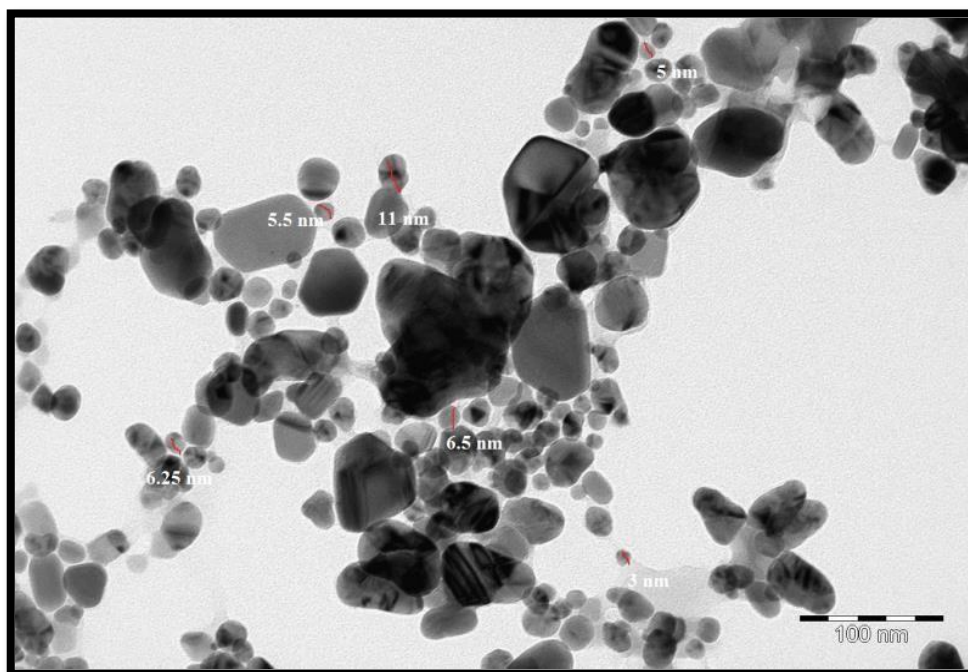


Figure 7- TEM image of silver nanoparticles at pH 7 with stirring and heating at 70 C° for one hour.

The FT-IR analysis was utilized to identify the different functional groups present in *L. Rosa* flowers extract, which can be responsible for the reduction of AgNO_3 to silver nanoparticles and play roles as efficient capping and stabilization agents. Figure-8 shows a typical FT-IR spectrum for *L. Rosa* flowers extract along with a comparison with Figure-9 which shows AgNPs synthesized using this extract. Comparison of these two spectra indicated that the peak appears at 1514 cm^{-1} , which corresponds to alkene groups that were shifted to 2945 cm^{-1} . A peak corresponding to the azo group at $(1461-1625) \text{ cm}^{-1}$ was shifted to $(3255-3301) \text{ cm}^{-1}$ which corresponds to the formation of the amino group with increased intensity, indicating the binding of silver ion with the hydroxyl, azo, and amide groups of the flowers extract.

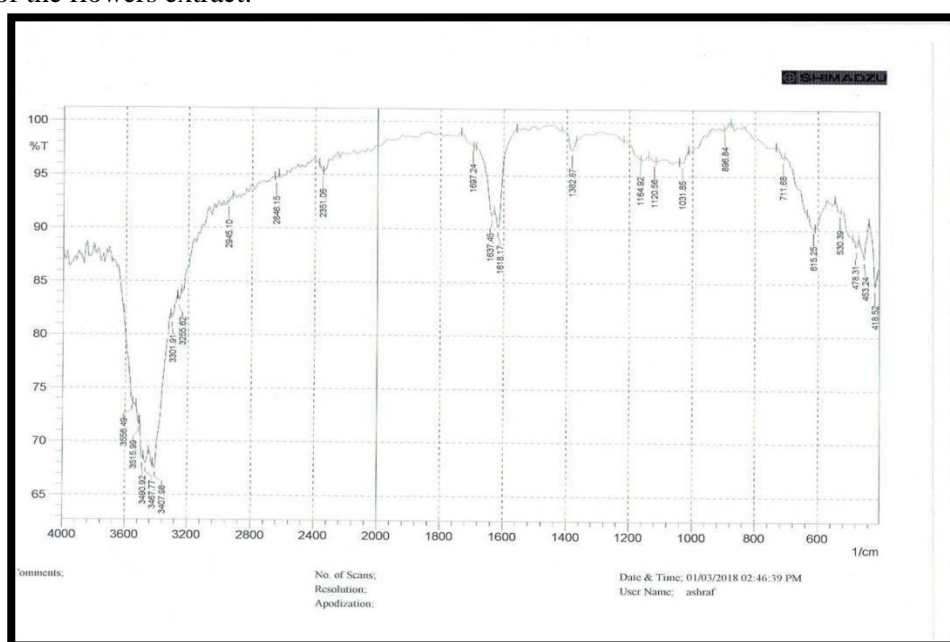


Figure 8- FT-IR spectrum for *L. rosa* flowers extract at pH 7 with stirring and heating at 70 C° for one hour.

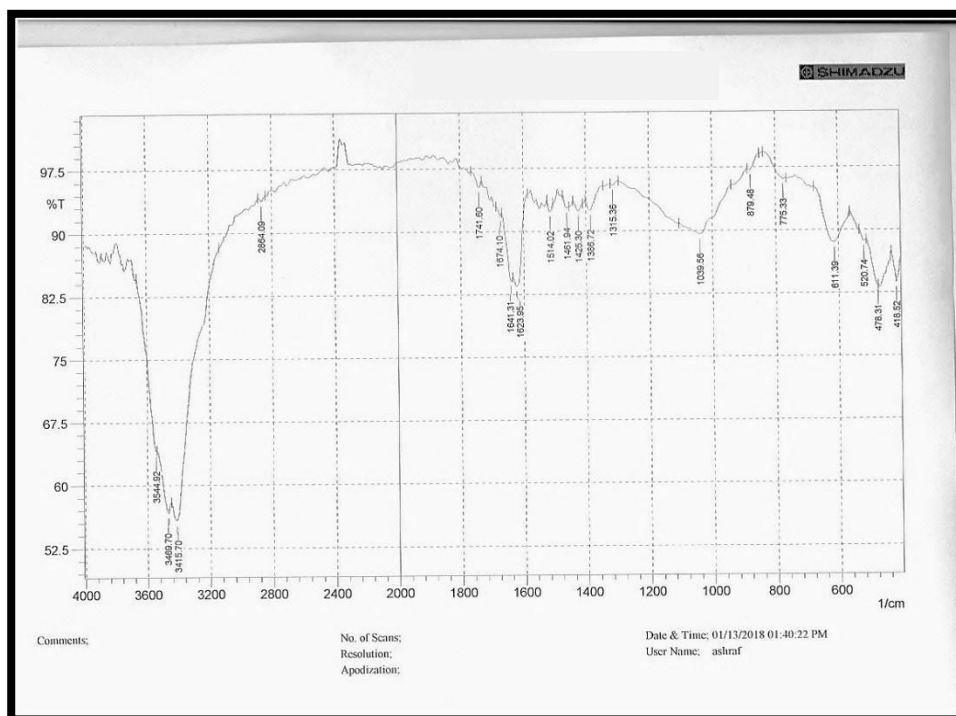


Figure 9- FT-IR spectrum of silver nanoparticles synthesized by *L. rosa* flowers extract at pH 7 with stirring and heating at 70 °C for one hour.

Atomic force microscope was used to present the surface morphology and to determine topography of the prepared NPs. AFM gives a three dimensional image of the surface of a nanoparticle. The particle diameter was calculated in nanoscale size, and the results demonstrated a diameter range of 20-50 nm. Figure- 10 shows the three-dimensional image of synthesized AgNPs using *L. rosa* flowers extract.

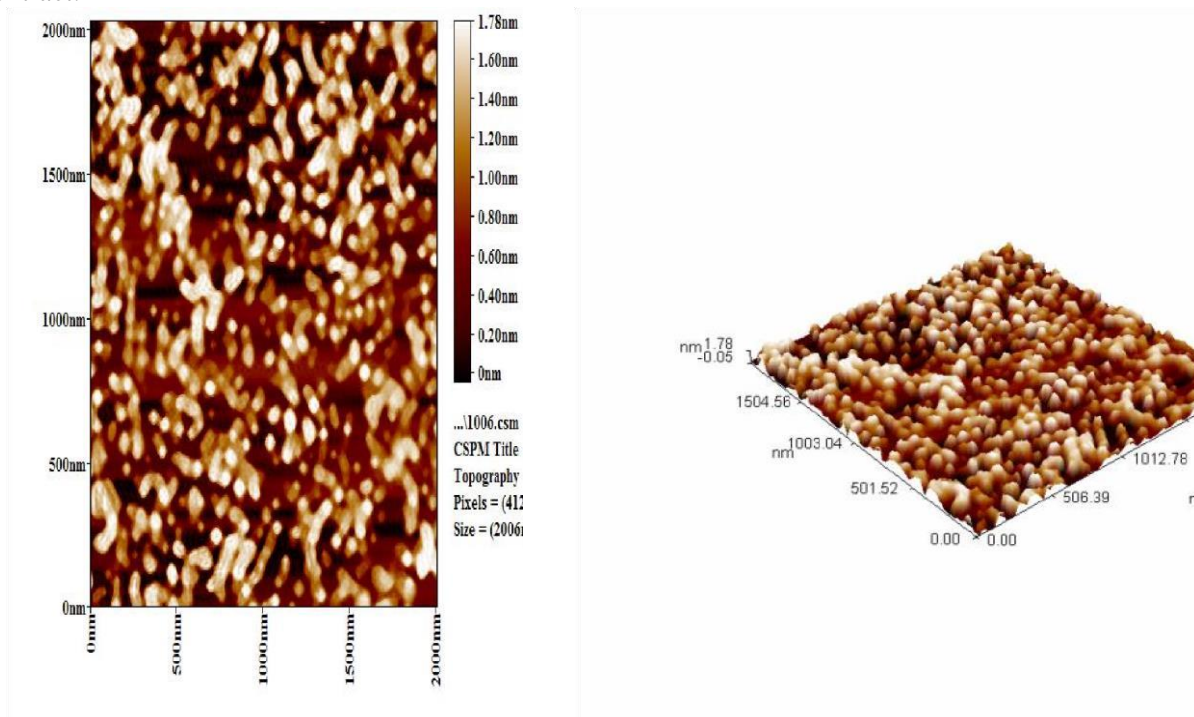


Figure 10- AFM image for the synthesized silver nanoparticles using *L. rosa* flowers extract at pH 7 with stirring and heating at 70 C° for one hour.

SEM images were used to show the size, shape and distribution of the synthesized silver nanoparticles. As shown in Figure-11, the particles are spherical with an average size between 10.5 to 74 nm.

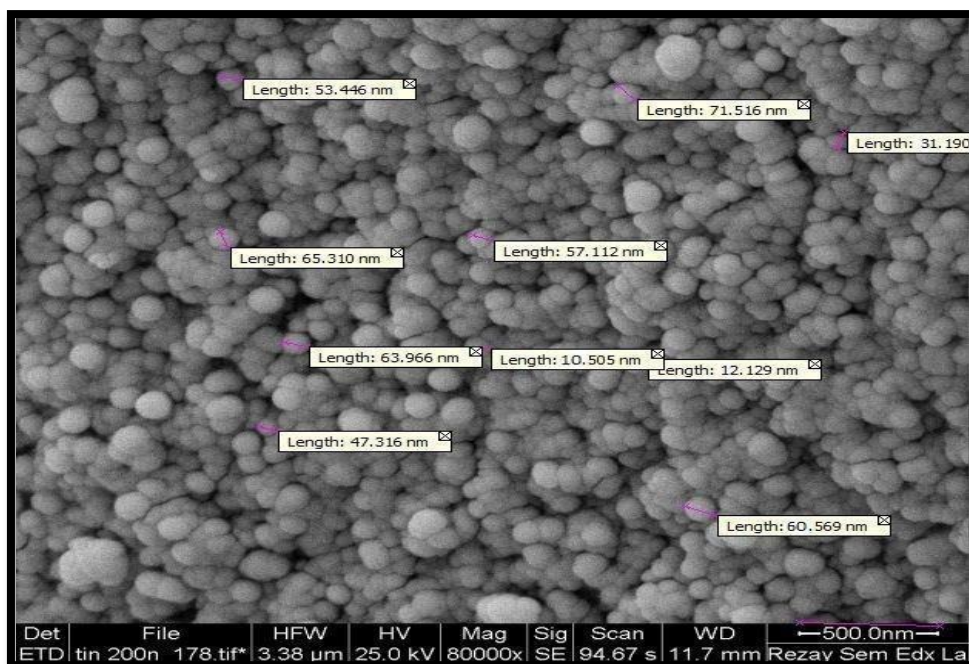


Figure 11- SEM image of silver nanoparticles prepared with *L. rosa* flowers extract at pH 7 with stirring and heating at 70 C° for one hour.

X-ray diffraction pattern showed four diffraction peaks at 38.12°, 44.25°, 65° and 78.45°, which are related to the planes 111, 200, 220 and 311, respectively, of the cubic structure silver. The lattice constant value calculated from this pattern was equal to 1.54180 Å, determined according to JCPDS (Joint Committee on Powder Diffraction Standards) NO. 04-0783. The average crystalline size of the silver nanoparticles formed in the bio-reduction process was determined by the application of Scherrer's formula, $d = (0.9 \lambda \times 180^\circ) / \beta \cos \theta \pi$, and was estimated to be 15.21 nm (Figure-12).

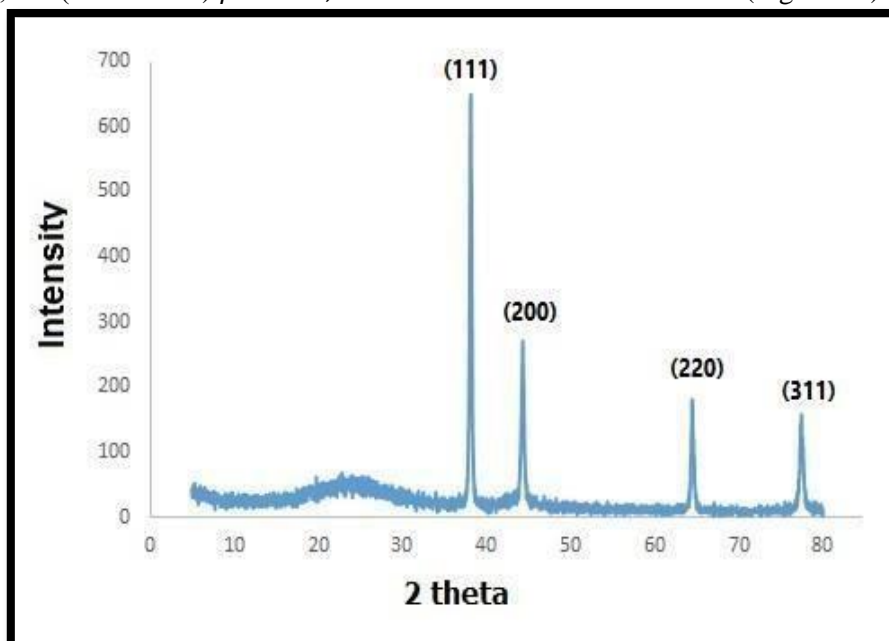


Figure 12- XRD pattern of silver nanoparticles synthesized using *L. rosa* flowers extract at pH 7 with stirring and heating at 70 C° for one hour.

Antibacterial effects of synthesized silver nanoparticles

The antimicrobial activity of the synthesized silver nanoparticles against gram negative *E. coli* and gram positive *Staphylococcus aureus* bacteria were revealed and the zone of inhibition was measured, as shown in Figure-13 and Table-1.

The results indicated that different concentrations of the synthesized silver nanoparticles showed effective antibacterial activities, both in gram negative and gram positive bacteria. Many studies confirmed that effect of silver nanoparticles on bacteria by destructing the membrane integrity [24, 25]. These studies indicated that silver nanoparticles may interact with phosphorus and sulphur-containing compounds, which may cause destruction to the DNA and proteins and, eventually, cell death. Based on the outcomes of this study, it is clear that silver nanoparticles may have significant applications in the agricultural sector and also could be sufficiently used as an effective agent against human pathogens [26]. AgNPs can easily penetrate bacteria through sulfate groups of the membrane protein resulting in the destruction of the structural composition of the bacteria. Also, AgNPs can pass into the cytoplasmic fluid where enzymatic proteins damaging could be occurred [27].

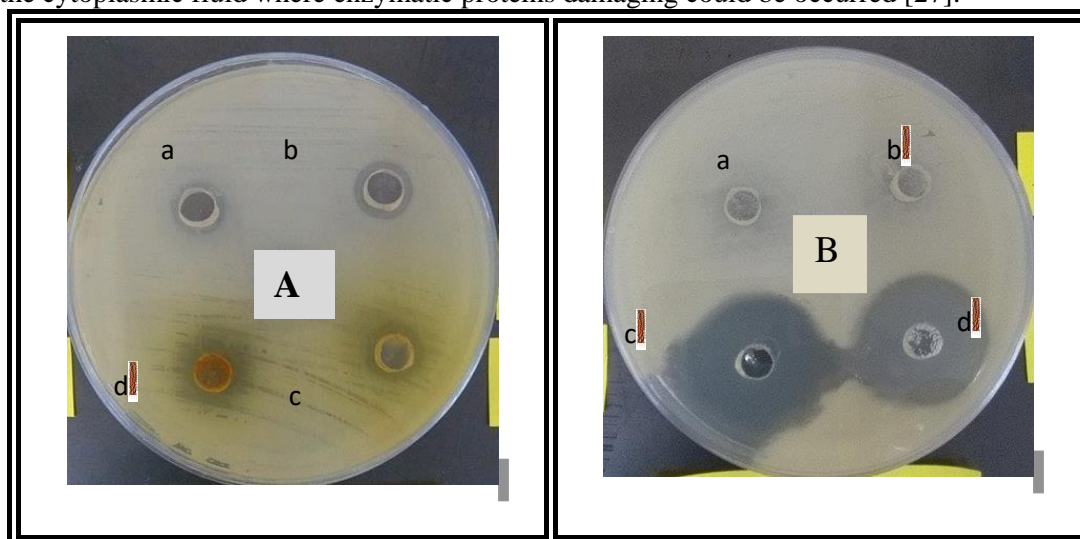


Figure 13-Antibacterial activity for synthesized AgNPs using different concentration of *L. rosa* flowers extract against (A) *E.coli* and (B) *Staphylococcus*; a) control, b) 1 mL, c) 1.5 mL, d) 2 mL *L. rosa* extract

Table 1- Diameters of zone of inhibition (millimeter) caused by different concentrations of AgNPs synthesized using *L. rosa* flowers extract against pathogenic bacteria.

Organism	Inhibition zone diameter (mm)			
	AgNPs (1 ml)	AgNPs (1.5 ml)	AgNPs (2 ml)	<i>L. rosa</i> flowers extract
<i>E-coli</i>	8	18	20	0.0
<i>Staphylococcus</i>	10	24	26	0.0

Impacts of silver nanoparticles on the activity of creatine kinase

The effects of AgNPs on the activity of creatine kinase are shown in Table-2 for both myocardial infarction patient and control groups. It is obvious that AgNPs have inhibition effects on CK activity. The inhibition percentage values of CK were (84%) and (74.7%) for the patient and control groups, respectively, as shown in Table-2. This decrease in CK activity might be due to the interaction between AgNPs and the thiol group of the amino acids (e.g. cysteine) found in the enzyme structure [28].

Table 2- Effects of silver nanoparticles on the activity of creatine kinase in the serum of patients with myocardial infarction

Activity of enzyme	Control group	Patient group
CK activity without AgNPs (U/L)	98.3	1263.3
CK activity (U/L) with AgNPs	16.6	99.9
Percent of inhibition	(74.7%)	(84%)

Kinetic and thermodynamic studies

The analysis of creatine kinase binding data was performed using Lineweaver-Burk equation. The activity of the enzyme was reduced in the presence of AgNPs. AgNPs bind equally well to the enzyme whether or not it has already bound to the substrate. V_{max} , K_m and K_{eq} values were calculated using Lineweaver-Burk equation (1):

$$\frac{1}{V} = \frac{K_m}{V_{max}} \cdot \frac{1}{[S]} + \frac{1}{V_{max}} \quad \dots\dots\dots(1)$$

Table 3- V_{max} , K_m and K_{eq} of creatine kinase in the serum of patients with myocardial infarction in the presence and absence of silver nanoparticles.

Group	V_{max} (U/L)	K_m (mM)	K_{eq} (mM ⁻¹)
Control	333.3	99.9	0.010
AgNPs-control	128.2	97.4	0.010
Patient	1666.6	55	0.018
AgNPs-patient	1000	72	0.013

ΔH values were unaffected by temperature, as they were constant over the range of temperatures used in this study. They were also positive for all studied groups, as shown in Table-4, indicating exothermic binding reaction between the enzyme and its substrate via the formation of sets of non-covalent interactions that yielded stabilization to the formed structure of enzyme-substrate complex. The association of CK from all studied groups to its substrate seems to proceed spontaneously in view of ΔG° values shown in Table-4. Values of this reaction depend on the molecular pathways of the mechanism of transformation [28].

The results also reveal the positive values of ΔS° , which indicates that the change from the order to the disorder state may be the driving force behind the reaction, which is observed to be unfavored by enthalpy but entropically favored. The differences seen in the value of ΔS° among the studied groups are a good indication of variation in their conformational stability, molecular flexibility, complexity and structure rigidity [29, 30].

Table 4- Results of the thermodynamic parameters of creatine kinase -catalyzed reaction at different temperatures of standard state for control, AgNPs-control, patients and AgNPs-patients groups

Temperature (C°)	ΔH° (j.mole ⁻¹)	ΔG° (j.mole ⁻¹)	ΔS° (j.mole ⁻¹)
Control			
20	177088.2	-828.2	177091
30	177088.2	-5340.4	177105.8
37	177088.2	-11855.5	177126.4
45	177088.2	-790511.7	179574.1
Control-AgNPs			
20	151314.8	-657.7	151317
30	151314.8	-5340.4	151332.4
37	151314.8	-10077.2	151347.3
45	151314.8	-502.322	151316.4
Patient			
20	168774.2	-1315.4	168778.7
30	168774.2	-3929.7	168787.2
37	168774.2	-11855.5	168812.4
45	168774.2	-131092.8	169186.4
Patient-AgNPs			
20	174178.3	-998.7	174181.7
30	174178.3	-2166.4	174185.4
37	174178.3	-11855.5	174216.5
45	174178.3	-12161.48	174216.5

Conclusions

In the present study, AgNPs were synthesized with greater stability and good yield, using simple, cheap and environmentally green method. This single step procedure is more suitable for large scale production, as it is rapid and eliminates the elaborate processes employed in the other bio-based protocols (e.g. by using fungi and bacteria). Interestingly, silver nanoparticles revealed good anti-bacterial activities at relatively low concentration. Based on the present findings, it is concluded that silver nanoparticles could be used as anti-bacterial agents in controlling different pathogens. However, it is necessary to conduct further studies to understand the exact mechanisms by which silver nanoparticles enter into the cell wall of bacterial. Silver nanoparticles showed a decrease in creatine kinase activity. The kinetic study showed that the inhibition type was noncompetitive, whereas the thermodynamic study revealed exothermic enthalpy, spontaneous Gibbs free energy, and change from order to disorder of entropy for all study groups.

Acknowledgments

The authors would like to acknowledge prof. Suaad M. Hussain for her valued assistance in FT-IR spectra explanations. This work was a part of an MSc. thesis at the University of Baghdad / College of Science / Department of Chemistry.

References

1. Arakelyan S, et al. **2016**. Reliable and well-controlled synthesis of noble metal nanoparticles by continuous wave laser ablation in different liquids for deposition of thin films with variable optical properties. *Journal of Nanoparticle Research*, **18**(6):155.
2. Mohammed MA, Rheima AM, Jaber SH, & Hameed SA. **2020**. The removal of zinc ions from their aqueous solutions by cr2o3 nanoparticles synthesized via the uv-irradiation method. *Egyptian Journal of Chemistry*, **63**(2):425-431.
3. Rheima AM, Mohammed MA, Jaber SH, & Hameed SA. **2019**. Synthesis of silver nanoparticles using the uv-irradiation technique in an antibacterial application. *Journal of Southwest Jiaotong University*, **54**(5).
4. Okafor F, Janen A, Kukhtareva T, Edwards V, & Curley M. **2013**. Green synthesis of silver nanoparticles, their characterization, application and antibacterial activity. *International journal of environmental research and public health*, **10**(10):5221-5238.
5. Baghayeri M, Mahdavi B, Hosseinpor-Mohsen Abadi Z, & Farhadi S. **2018**. Green synthesis of silver nanoparticles using water extract of salvia leriifolia: Antibacterial studies and applications as catalysts in the electrochemical detection of nitrite. *Applied Organometallic Chemistry*, **32**(2):e4057.
6. Garibo D, et al. **2020**. Green synthesis of silver nanoparticles using lysiloma acapulcensis exhibit high-antimicrobial activity. *Scientific reports*, **10**(1):1-11.
7. Burduşel A-C, et al. **2018**. Biomedical applications of silver nanoparticles: An up-to-date overview. *Nanomaterials*, **8**(9):681.
8. Ahmed RH & Mustafa DE. **2020**. Green synthesis of silver nanoparticles mediated by traditionally used medicinal plants in sudan. *International Nano Letters*, **10**(1):1-14.
9. Logeswari P, Silambarasan S, & Abraham J. **2015**. Synthesis of silver nanoparticles using plants extract and analysis of their antimicrobial property. *Journal of Saudi Chemical Society*, **19**(3):311-317.
10. Khatoon N, Mazumder JA, & Sardar M. **2017**. Biotechnological applications of green synthesized silver nanoparticles. *J. Nanosci. Curr. Res*, **2**:107.
11. Bhatt DL, Topol EJ, CUTLIP DE, & KUNTZ RE **2005**. Does creatinine kinase-mb elevation after percutaneous coronary intervention predict outcomes in 2005? Authors' reply. *Circulation (New York, NY)* **112**(6):906-923.
12. Paula MMdS, et al. **2009**. In vitro effect of silver nanoparticles on creatine kinase activity. *Journal of the Brazilian Chemical Society* **20**(8):1556-1560.
13. Huang W, Zhang Y, Bao S, Cruz R, & Song S. **2014**. Desalination by capacitive deionization process using nitric acid-modified activated carbon as the electrodes. *Desalination*, **340**:67-72.
14. AL-Rufaie M & AL-Zubaidi HY. **2018**. Biosynthesis of silver nanoparticles using (carissa macrocarpa) leaves extract and study its antibacterial activity. -1:) 46(3 *The Middle East Journal* **22**.
15. Elamawi RM, Al-Harbi RE, & Hendi AA. **2018**. Biosynthesis and characterization of silver nanoparticles using trichoderma longibrachiatum and their effect on phytopathogenic fungi. *Egyptian journal of biological pest control*, **28**(1):28.
16. Li H, Burrow MF, & Tyas MJ. **2003**. The effect of concentration and ph of silver nitrate solution on nanoleakage. *Journal of Adhesive Dentistry*, **5**(1).
17. Baharara J, Namvar F, Ramezani T, Hosseini N, & Mohamad R. **2014**. Green synthesis of silver nanoparticles using achillea biebersteinii flower extract and its anti-angiogenic properties in the rat aortic ring model. *Molecules*, **19**(4):4624-4634.
18. Magaldi S, et al. **2004**. Well diffusion for antifungal susceptibility testing. *International journal of infectious diseases*, **8**(1):39-45.
19. Manikandan DB, et al. **2021**. (Green fabrication, characterization of silver nanoparticles using aqueous leaf extract of ocimum americanum (hoary basil) and investigation of its in vitro

- antibacterial, antioxidant, anticancer and photocatalytic reduction. *Journal of Environmental Chemical Engineering* , **9**(1):104845.
20. Glick N, Landman A, & Roufogalis B. **1979**. Correcting lineweaver-burk calculations of v and k m. *Trends in Biochemical Sciences*, **4**(4):N82-N83.
 21. Lima EC, Gomes AA, & Tran HN. **2020**. Comparison of the nonlinear and linear forms of the van't hoff equation for calculation of adsorption thermodynamic parameters (Δs° and Δh°). *Journal of Molecular Liquids*:113315.
 22. Zook JM, Long SE, Cleveland D, Geronimo CLA, & MacCuspie RI. **2011**. Measuring silver nanoparticle dissolution in complex biological and environmental matrices using uv-visible absorbance. *Analytical and bioanalytical chemistry*, **401**(6):1993.
 23. Selimovic V, et al. **2018**. Aerosol optical properties and trace gas emissions by pax and opftir for laboratory-simulated western us wildfires during firex.
 24. Asghar MA, et al. **2018**. Iron, copper and silver nanoparticles: Green synthesis using green and black tea leaves extracts and evaluation of antibacterial, antifungal and aflatoxin b1 adsorption activity. *LWT* 90:98-107.
 25. Baker S, Kumar KM, Santosh P, Rakshith D, & Satish S. **2015**. Extracellular synthesis of silver nanoparticles by novel pseudomonas veronii as41g inhabiting annona squamosa l. And their bactericidal activity. *Spectrochimica Acta Part A: Molecular and Biomolecular Spectroscopy* **136**:1434-1440.
 26. Halawani EM. **2016**. Rapid biosynthesis method and characterization of silver nanoparticles using zizyphus spina christi leaf extract and their antibacterial efficacy in therapeutic application. *Journal of Biomaterials and Nanobiotechnology* , **8**(1):22-35.
 27. Pourmortazavi SM, Taghdiri M, Makari V, & Rahimi-Nasrabadi M. **2015**. Procedure optimization for green synthesis of silver nanoparticles by aqueous extract of eucalyptus oleosa. *Spectrochimica Acta Part A: Molecular and Biomolecular Spectroscopy* , **136**:12491254.
 28. Batista JAD. **2017**. Estudo do encapsulamento de compostos DNA-fármacos por um polipeptídeo recombinante.
 29. Suhail GT, Anter FH, & Al-Sarraj ZS. **2018**. Study the of effect of micro and nanocadmium oxide on the hardness test of (epoxy-polyurethane) blend. *Iraqi Journal of Science*:2020-2025.
 30. Alwan AM, Mohammed MS, & Shehab RM. **2020**. The performance of plasmonic gold and silver nanoparticle-based sers sensors. *Iraqi Journal of Science*:1320-1327.